In Silico and Validation Approaches for Optimum Conditions of Rattus norvegicus Target Gene qPCR Primers

by Firman Alamsyah

Journal of Tropical Biodiversity and Biotechnology
Volume 08, Issue 02 (2023): jtbb71765
DOI: 10.22146/jtbb.71765

Research Article

In Silico and Validation Approaches for Optimum Conditions of *Rattus norvegicus* Target Gene qPCR Primers

Gracia Alice Victoria Pollo[1], Nyoman Yudi Antara[2], Firman Alamsyah[3], Rarastoeti Pratiwi[1]*
1)Faculty of Biology, Universitas Gadjah Mada, Yogyakarta, 55281, Indonesia
2)Faculty of Health, Universitas Kader Bangsa, Palembang, 30129, Indonesia
3)Center for Medical Physics and Cancer Research, CTECH Laboratories EDWAR TECHNOLOGY, Tangerang, 15320, Indonesia
* Corresponding author, email: rarastp@ugm.ac.id

Keywords:
experimental validation
in silico
oligonucleotide
qPCR primer
SYBR Green I
Submitted:
31 December 2021
Accepted:
07 March 2023
Published:
05 June 2023
Editor:
Ardaning Nuriliani

ABSTRACT
Gene expression analysis using the qPCR method requires an oligonucleotide pair to prime the amplification process. Supporting the widely used qPCR method, variety of qPCR reagents and primer options are available. This infers to the importance of *in silico* and laboratory experimental validation approach considering SYBR Green optimum annealing temperature to validate the most suitable primer for prior use. Several genes are suspected to be involved in the BM-MSCs migration and differentiation into Cancer-associated Fibroblast Cells in *Rattus norvegicus*. This article aims to provide *in silico* analysis with the case of the suspected genes namely actin alpha-2 smooth muscle (*ACTA2*), fibroblast activation protein (*FAP*), hypoxanthine phosphoribosyltransferase-1 (*HPRT1*), platelet-derived growth factor subunit B (PDGFB), phosphoinositide-3-kinase regulatory subunit-1 (*PIK3R1*), and vascular cell adhesion molecule-1 (*VCAM1*) qPCR primer with qPCR and electrophoresis validation. The procedure used in this approach was *in silico* analysis of primer from published articles and newly designed primer. The analysis was done with Primer-BLAST for gene specificity, Primer-Dimer, OligoCalc for hairpin formation, BLAST Nucleotide for identical sequence screening, and Clustal Omega for product length validation. Experimental validation was done using qPCR for optimal annealing temperature, priming ability, amplicon specificity, and electrophoresis for product length validation. This assessment resulted in *in silico* and laboratory experimental validation of *ACTA2*, *FAP*, *HPRT1*, *PDGFB*, *PIK3R1*, and *VCAM1* primer pairs producing suitable amplicon for qPCR using *Rattus norvegicus* cDNA with SYBR annealing temperature range of 60-65° C with three mM $MgCl_2$. The primer pairs can be used for further qPCR analysis under similar conditions and the procedure stated can be used as starting point for qPCR Primer preparation accounting for fluorophore optimum annealing temperature.

INTRODUCTION
A molecular approach such as qPCR has been the vastly used method (Luna et al. 2012; Canh et al. 2020; Caselli et al. 2021) . This approach has been applied to various gene expression analyses (Fiechter et al. 2021; Sharma et al. 2021), pathological detection (Caselli et al. 2021), and

microbial detection (Luna et al. 2012; Cuevas-Ferrando et al. 2021). Broad options for qPCR reagent are offered (Petrovan et al. 2020; Brown et al. 2021; Yang et al. 2021) with broad options of analysis object present (Luna et al. 2012; Fiechter et al. 2021).

A variety of qPCR reagents having different reaction conditions can affect the annealing of primer, where a pair of oligonucleotides is required to prime the amplification process (Sato et al. 2021). Research showed that even SYBR Green I was used by several different manufacturers, there would still be variations in the amplification (Hargreaves et al. 2013). $MgCl_2$ concentration is known to give a slight change in annealing temperature. Annealing temperatures from the same set of primer can affect amplification (Hargreaves et al. 2013). The prediction that can be done for primer can give the researchers chance to bypass designing primer pairs with the unintended annealing possibility (Johnston et al. 2019). Most available primers on published articles share a wide range of melting temperatures. It presents challenges in using those primers with the possible different reagents (Vogels et al. 2020; Yang et al. 2020; Langlois et al. 2021). Prior to qPCR primers application, *in silico* (Vanneste et al. 2018; Covey 2021) and laboratory experimental approach (Trigo et al. 2021) are essential in validating the most suitable primer.

Several suspected genes are involved in the BM-MSCs migration and differentiation into cancer associated fibroblast (CAF) cells in *Rattus norvegicus*' breast tumour. A chemoattractant gene, *PDGFB*, is involved in that migration (Camorani et al. 2017). Genes such as *PIK3R1* (Jiménez et al. 2000) and *VCAM1* (Hu et al. 2012) are involved in cellular migration signalling process. *ACTA2* and *FAP* are the genes expressing CAFs molecular markers (Costa et al. 2018). Prior to relative gene expression analysis on *Rattus norvegicus* gene expression, qPCR primer for *ACTA2*, *FAP*, *HPRT1*, *PDGFB*, *PIK3R1*), and *VCAM1* had been analyzed. Due to the specificity of SYBR efficacy to function, this article shares the evidence about the analyzed qPCR primers producing suitable primer pairs for SYBR Green I with three mM of $MgCl_2$.

MATERIALS AND METHODS

Materials

In silico materials used were Google Scholar search engine, National Center for Biotechnology Information (NCBI) database, and software tool (Primer3, Primer-Blast, Primer-Dimer, OligoCalc, Nucleotide Blast, Clustal Omega). Laboratory experimental validation materials used were *Rattus norvegicus* cDNA (ethical clearance: No. 00029/04/LPPT/IV/2018), nuclease-free water (Thermo Scientific Water Nuclease-Free R0581), qPCR reagent (Bioline SensiFAST SYBR No-ROX Kit BIO-98005), qPCR primer (synthesized by Integrated DNA Technologies (IDT)), agarose powder, Tris-Boric-EDTA (TBE) buffer (1st BASE – 10X TBE Buffer BUF-3010-10X1L), DNA Ladder (Smobio ExcelBandTM 100bp DNA Ladder DM1100), microtube (Biologix), qPCR tube (Biorad – 0.2 mL 8-tube PCR strips without caps, low profile, white – TLS0851), qPCR tube lid (BioRad – 0.2 mL flat PCR tube 8-cap strips optical, ultra-clear – JH95290002), micropipette tip (Biologix), and parafilm (Parafilm "M" Roll Size Four in x 125 ft – P7793 – 1EA).

Methods

Primer sequences for all targeted genes were searched in related published articles throughout Google Scholar Search Engine and articles citing the curated mRNA database accession numbers in National Center for Biotechnology Information (NCBI) database. This was accessed through NM_031004.2 for *ACTA2* mRNA sequence, NM_138850.1 for *FAP* mRNA sequence, NM_012583.2 for *HPRT1* mRNA sequence, NM_031524.1 for *PDGFB* mRNA sequence, NM_013005.2 for *PIK3R1* mRNA sequence, and NM_012889.2 for *VCAM1* mRNA sequence. The decision of unsuitable primer was based on Primer3 analysis, particularly on melting temperature outside the favourable melting temperature range by the manufacturer, which was 60-65°C. The suitable primer sets went through further procedures for *in silico* analysis. Primer pairs from published articles with unsuitable results were decided to be designed based on the database. The analyzed primers were then synthesized and underwent laboratory experimental validation.

In silico design and analysis

A. Primer3

Primer design was done using Primer3 as suggested by the Bioline SYBR qPCR kit. This bioinformatics tool was accessed through http://frodo.wi.mit.edu/primer3/. Primer set sequences from published articles were submitted for analysis. The FASTA sequences of the stated accession numbers were used as the primer design template. The product size range used was 80-200 bp as suggested. Primer Tm preferences were set in accordance with the qPCR kit's recommendations. The minimum primer Tm was set to 60.0°C. The optimal primer Tm was set to 62.5°C as the median point. The maximum primer Tm was set to 65.0°C. The maximum primer Tm difference was set to 1°C.

B. Primer Blast

Primer specificity was analyzed using PrimerBLAST (Ye et al. 2012). This bioinformatics tool was accessed through https://www.ncbi.nlm.nih.gov/tools/primer-blast/. The designed primer set sequences in the 5'-3' direction were submitted. The organism's name was specified for the targeted organism sample. Other parameters were left unedited because the primer set sequences were already determined as this approach was used for analyzing gene specificity. The primer set was determined as gene-specific when the primer set was only specific to the desired gene.

C. Primer Dimer

The possibility of primer dimer formation was analyzed by using Primer Dimer by Primer Suite. Primer Dimer's website was accessed at http://www.primer-dimer.com/. The forward and reverse primer sequences were submitted in FASTA format. Paired analysis was used for dimer possibility formation screening between forward and reverse primers. Result output option of 'Dimer Structure Report' was chosen for the predicted most stable dimer formation.

D. Primer Hairpin

The possibility of primer hairpin formation was analyzed by using OligoCalc through http://biotools.nubic.northwestern.edu/OligoCalc.html. Primer set sequences were submitted separately. The separate input was done due to the hairpin formation being a self-complementary formation, thus the analyses were done separately.

E. Nucleotide Blast

Primer specificity validation was done by using BlastNucleotide through https://blast.ncbi.nlm.nih.gov/Blast.cgi?PROGRAM=blastn&PAGE_TYPE=BlastSearch&LINK_LOC=blasthome. Forward and reverse primer sequences were submitted separately. The reverse primer sequence underwent 'Reverse-Complement' formatting through https://www.bioinformatics.org/sms/rev_comp.html before submission. The sample organism was then used to filter the result for organism specificity.

F. Clustal Omega

Primer product length validation was done by using 'Clustal Omega'. This alignment tool was accessed through https://www.ebi.ac.uk/Tools/msa/clustalo/. The 'DNA' option was chosen as the sequence type. Fasta sequences of the primer set and similar sequences from Blast Nucleotide were submitted. The primer set sequences were validated to be conserved with the reference target sequences. The number of nucleotides covered from forward primer to reverse primer was counted and validated to the expected amplicon length.

In-lab validation

A. Primer annealing temperature optimization

Primer annealing temperature optimization was done by using CFX96 Touch Real-Time PCR System. The reaction consisted of 5 µL SYBR Green reagents, 3.2 µL nuclease-free water, 0.4 µL 10 µM forward primer, 0.4 µL 10 µM reverse primer, 1 µL cDNA (25 ng of the corresponding RNA) of *Rattus norvegicus*, Sprague Dawley Strain. The reaction was carried out as stated in the manufacture's protocol. Gradient temperatures used for annealing temperature optimization were 61.0; 61.8; 62.6; 63.6; and 64.8°C, each with two replicate reactions. These two replications for each temperature aimed for result reproducibility.

B. Electrophoresis

Electrophoresis was needed to be done for amplicon length validation as bioinformatically estimated. The 2% electrophoresis gel was prepared with 1x TBE as solvent and running buffer. DNA ladder (5 µL) was loaded into the gel well. The 5 µL amplified samples with 1 µL loading dye were loaded into the gel well. The electrophoresis process was done by using 110 V for 25 minutes. The gel was then visualized using a UV transilluminator.

RESULTS AND DISCUSSION

Results

ACTA2 Primer

The analyzed primers from published articles were considered unsuitable for favourable temperature ranges. Primer design targeted for *ACTA2* using NM_031004.2 sequence resulting in various primer sets. One set of the resulting primers were 5'-GCCATCATGCGTCTGGACTT-3' for forward primer and 5'-CTCACGCTCAGCAGTAGTCACG-3' for reverse primer. The calculated melting temperature was 63.53°C for forward primer and 63.57°C for reverse primer. The melting temperature difference was 0.04°C. The GC contents of the primer set were 55% for forward primer and 59.09% for reverse primer. The gene specificity analysis resulted in specific targeting of *ACTA2* mRNA of *Rattus norvegicus* mRNA database (Figure 1a). It showed no possibility of an unintended priming site on the other genes in the targeted animal sample. The specific *ACTA2* primer pair was further analyzed for primer dimer. The analysis showed a possibility of primer dimer formation at the end of reverse with two hydrogen bonds (Figure 1b). The subsequent analysis processes were still carried on considering overall results that needed to be determined. Primer hairpin possibilities analysis showed that both forward and reverse primers had no possibilities for primer hairpin formation. The primer set has two identical sequences for both primer sequences which were NM_031004.2 for the *Rattus norvegicus* curated *ACTA2* mRNA sequence and BC158550.1 for *Rattus norvegicus ACTA2* cDNA clone. The sequence alignment showed that the forward primer and reverse primer confine amplification to produce 102 bp amplicon which conformed to primer design information.

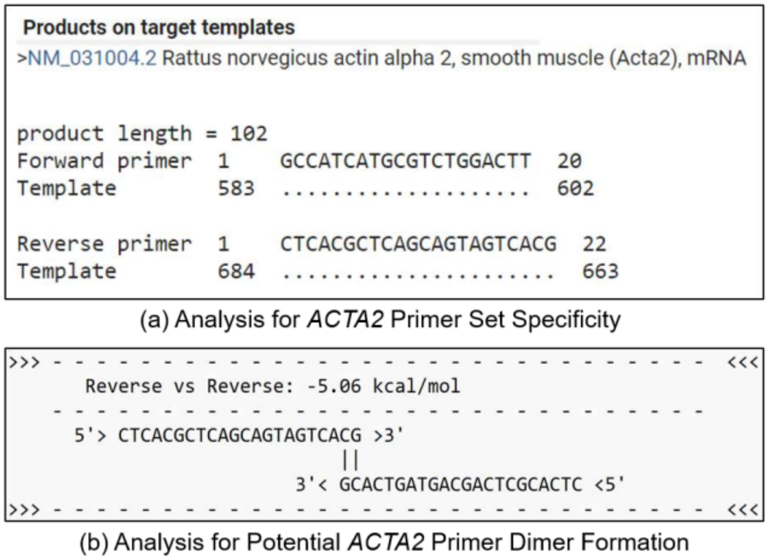

Figure 1. Bioinformatic Primer Analysis Results for *ACTA2* Primer. (a) Analysis result from Primer-Blast (https://www.ncbi.nlm.nih.gov/tools/primer-blast/) showed primer specificity to *ACTA2* mRNA. (b) Analysis result from PrimerDimer (http://www.primer-dimer.com/) showed low indication of Primer Dimer Formation with two hydrogen bonds.

The designed and bioinformatically analyzed primer set was further analyzed for its reliability using qPCR, electrophoresis, and NTC analysis. In general, the amplification chart showed that this primer could prime amplification (Figure 2a). The qPCR amplification result was followed by the qPCR melt curve and melt peak results. It showed that *ACTA2* primer amplification resulted in one specific dissociation (Figure 2b) and melt peak (Figure 2c) indicating specific priming for all annealing temperatures used. The temperature which produced the lowest Ct value indicated the most compatible temperature for *ACTA2* primer to anneal by having the appropriate condition to anneal resulting in higher amplicon products. The optimal annealing temperature for *ACTA2* primer was considered as 61°C dues to the lowest Ct value produced (Figure 2g). The qPCR products of *ACTA2* primer with the annealing temperature of 61°C were then used for electrophoresis-based product length validation. The visualized amplicon length corresponded to the DNA ladder of 100 bp (Figure 2h). It validated the bioinformatic analysis of the primer resulting in a 100 bp amplicon. The NTC reaction was run for *ACTA2* primer and the amplification chart (Figure 2d), melt curve (Figure 2e), and melt peak (Figure 2f) showed that there was no possibility of amplification of primer dimer. These overall results suggested that this primer set can be used for subsequent gene expression analysis.

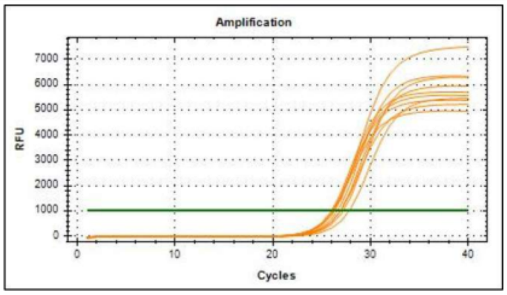

(a) Amplification Plot of *ACTA2* Primer Annealing Temperature Optimization

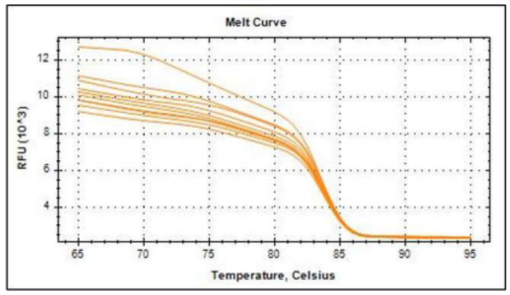

(b) Melt Curve of *ACTA2* Primer Annealing Temperature Optimization

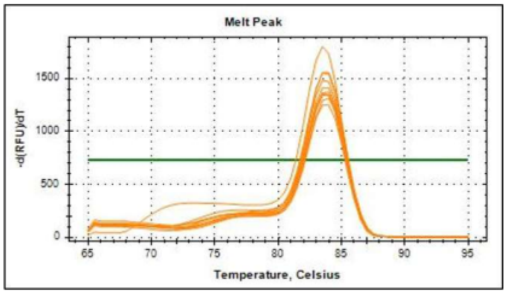

(c) Melt Peak of *ACTA2* Primer Annealing Temperature Optimization

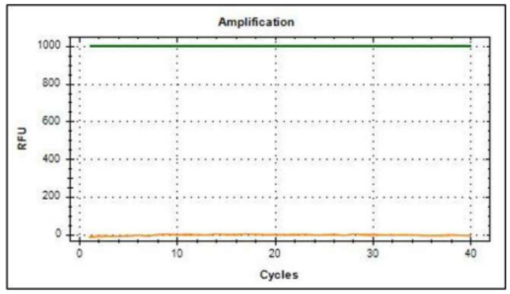

(d) Amplification Plot of *ACTA2* Primer NTC

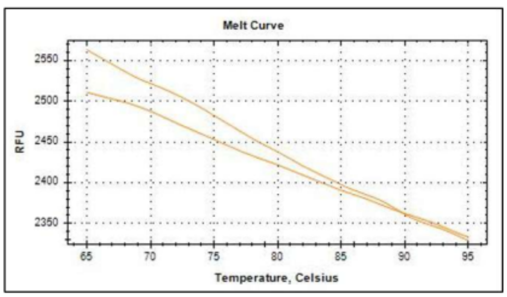

(e) Melt Curve of *ACTA2* Primer NTC

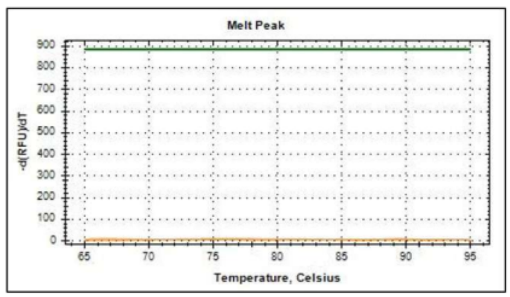

(f) Melt Peak of *ACTA2* Primer NTC

ACTA2				
Temperature (°C)	Ct1	Ct2	Ct Average	Ct Difference
64.8	27.22	27.85	27.535	0.63
63.6	26.95	27.02	26.985	0.07
62.6	26.33	26.63	26.48	0.3
61.8	26.21	26.18	26.195	0.03
61	26.05	26.16	26.105	0.11

(g) Ct Value of *ACTA2* Primer Annealing Temperature Optimization

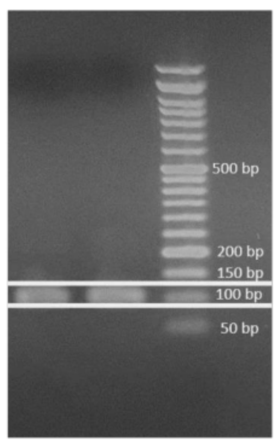

(h) Electrophoresis Validation on Product Length of *ACTA2* Primer

Figure 2. Experiment Validation using qPCR and Electrophoresis for *ACTA2* Primer. Results from qPCR run showed (a) successful amplification process, (b) specific dissociation of amplicons, (c) specific melt peak of amplicons, with no primer-dimer evident based on (d) no amplification, (e) no dissociation and (f) no melt peak from NTC reaction, (g) temperature gradient qPCR run showed the optimum annealing temperature with lowest Ct detected, (h) electrophoresis run showed specific amplicon with targeted length.

FAP Primer

Primer for *FAP* was screened throughout the published articles and then analyzed. The primer pair selections did not fit the bioinformatic criteria. Thus, qPCR primer for *FAP* was decided to be designed and screened for matching criteria. The suitable resulted in primer pair was 5'-TGTTTCATCCCTAGCCCTTGC-3' for forward primer and 5'-TGTTGGGAGGCCCATGAAT-3' for reverse primer. The calculated melting temperatures were 63.56°C for forward primer and 63.59°C for a reverse primer with the melting temperature difference of 0.03°C. The GC content for each primer was 52.38% for forward primer and 52.63% for reverse primer. The primer pair produced a 124 bp amplicon based on bioinformatic analysis on NM_138850.1. The accession number of NM_138850.1 is the accession number of *Rattus norvegicus* fibroblast activation protein alpha (*FAP*) mRNA. The primer pair was analyzed as specific to the target gene (Figure 3a). The primer pair was analyzed for primer dimer possibility. There was a possibility of primer dimer formation in two forward primer sequences with two hydrogen bonds at the end of the sequences (Figure 3b). Throughout the primer selections, both from reference articles and designed primers, this primer pair had the least possible primer dimer formation with no hairpin formation possibility. The primer pair was analyzed manually through nucleotide alignment and showed the product length was 124 bp corresponding to Primer3 and Primer Blast results.

```
Products on target templates
>XM_039104226.1 PREDICTED: Rattus norvegicus fibroblast activation protein, alpha (Fap), transcript variant X2, mRNA

product length = 124
Forward primer  1     TGTTTCATCCCTAGCCCTTGC  21
Template        2036  .....................  2056

Reverse primer  1     TGTTGGGAGGCCCATGAAT  19
Template        2159  ...................  2141

>XM_039104225.1 PREDICTED: Rattus norvegicus fibroblast activation protein, alpha (Fap), transcript variant X1, mRNA

product length = 124
Forward primer  1     TGTTTCATCCCTAGCCCTTGC  21
Template        2036  .....................  2056

Reverse primer  1     TGTTGGGAGGCCCATGAAT  19
Template        2159  ...................  2141

>NM_138850.1 Rattus norvegicus fibroblast activation protein, alpha (Fap), mRNA

product length = 124
Forward primer  1     TGTTTCATCCCTAGCCCTTGC  21
Template        1891  .....................  1911

Reverse primer  1     TGTTGGGAGGCCCATGAAT  19
Template        2014  ...................  1996
```

(a) Analysis for *FAP* Primer Set Specificity

```
>>> - - - - - - - - - - - - - - - - - - - - - - - - - - - - - - - - - - - <<<
      Forward vs Forward: -3.86 kcal/mol
    - - - - - - - - - - - - - - - - - - - - - - - - - - - - - - - - - - -
     5'> TGTTTCATCCCTAGCCCTTGC >3'
                             ||
                       3'< CGTTCCCGATCCCTACTTTGT <5'
>>> - - - - - - - - - - - - - - - - - - - - - - - - - - - - - - - - - - - <<<
```

(b) Analysis for Potential *FAP* Primer Dimer Formation

Figure 3. Bioinformatic Primer Analysis Results for *FAP* Primer. (a) Analysis result from Primer-Blast (https://www.ncbi.nlm.nih.gov/tools/primer-blast/)

showed primer specificity to *FAP* mRNA. (b) Analysis result from PrimerDimer (http://www.primer-dimer.com/) showed low indication of Primer Dimer Formation with two hydrogen bonds.

The selected primer pair was then tested for amplification priming ability with qPCR machine with annealing temperature optimization. The amplification chart showed that the primer pair could amplify the cDNA template (Figure 4a). The primed amplification with various annealing temperatures showed a slight difference in amplicon dissociation seen in the melt curve chart (Figure 4b) across annealing temperatures. The melt peak chart showed that the annealing temperature conditions of 61.0 and 61.8°C resulted in two possible amplicons. The otherwise happened to amplify with the annealing temperature condition of 62.6; 63.6; and 64.8°C. The three annealing temperature conditions resulted in one possible amplicon (Figure 4c). The lowest Cq value resulted from 61.0°C (Figure 4g) which might result in the optimal priming condition being refused to be one of the primer option considerations. It is because this annealing temperature has the possibility of facilitating the amplification for two amplicons rather than one specific amplicon. This can be seen by the two melt peaks in the melt peak curve. The possible annealing temperature for this primer pair was 63.6°C with the highest precision for annealing temperature producing one possible amplicon. The amplicon with one melt peak from annealing temperature of 63.6°C resulted in one electrophoresis visualization band in between 100 and 150 bp marker bands referring to a specific amplicon length of 124 bp (Figure 4h). The primer dimer validation was done by running the NTC reaction with this primer. The amplification (Figure 4d), melt curve (Figure 4e), and melt peak (Figure 4f) charts showed that there was no possibility of primer-dimer and hairpin formation based on NTC reaction.

HPRT1 Primer

The primer pair of *HPRT1* from (Landry et al. 2019) matched the NM_013005.2 sequence. The sequence of this primer was 5'-CTCATGGACTGATTATGGACAGGAC-3' for forward primer and 5'-GCAGGTCAGCAAAGAACTTATAGCC-3' for reverse primer. The melting temperature for this primer pair was 63.12°C for forward primer and 63.63°C for a reverse primer with a 0.51°C difference. The GC contents for this primer set were 48% for both forward and reverse primer. This primer was specific for *Rattus norvegicus*. *HPRT1* mRNA produces 123 bp amplicon (Figure 5a). Primer dimer formation analysis resulted in two hydrogen bonds formation possibilities on the reverse primers (Figure 5b). Hairpin formation analysis revealed that both forward and reverse primer could not form a hairpin structure. The screening in the *Rattus norvegicus* gene database revealed that both submitted sequence of the primer set was identical to NM_013005.2 and several similar sequences. The sequences were simultaneously aligned which validates the priming site of primers. The result revealed that the primer set confined the targeted amplification to produce a 123 bp amplicon.

The resulting amplification data showed that the designed primer set was able to prime amplification on every annealing temperature used (Figure 6a). The overall amplification using this primer set can be said to be specific based on the specific melt curve (Figure 6b) and melt peak (Figure 6c) obtained. The lowest Ct value of two qPCR technical replicate reactions and average Ct value was produced by amplification with the annealing temperature of 62.6°C (Figure 6g). The amplification results using 62.6°C annealing temperature was used for electrophoresis. The amplicon visualization band resided between 100 and 150 bp (Figure

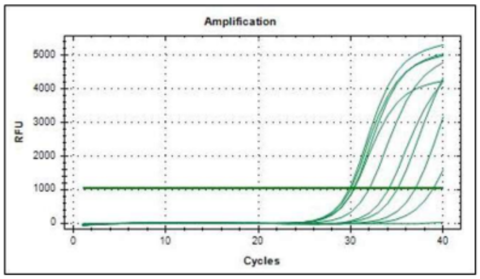

(a) Amplification Plot of *FAP* Primer Annealing Temperature Optimization

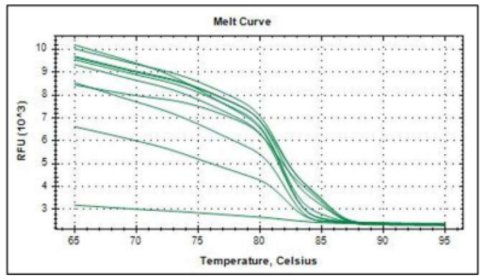

(b) Melt Curve of *FAP* Primer Annealing Temperature Optimization

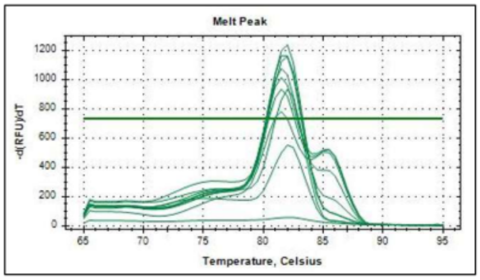

(c) Melt Peak of *FAP* Primer Annealing Temperature Optimization

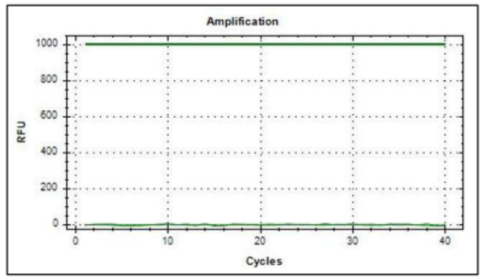

(d) Amplification Plot of *FAP* Primer NTC

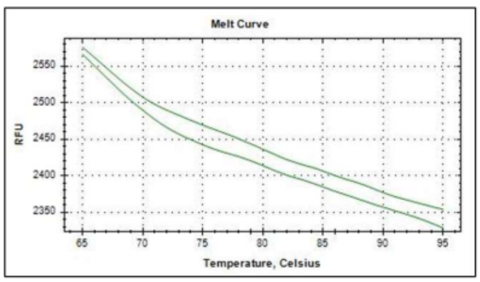

(e) Melt Curve of *FAP* Primer NTC

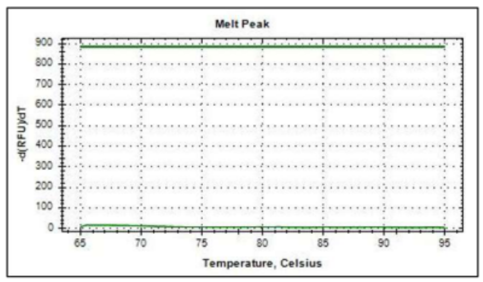

(f) Melt Peak of *FAP* Primer NTC

FAP				
Temperature (°C)	Ct1	Ct2	Ct Average	Ct Difference
64.8	37.02			
63.6	34.14	32.04	33.09	2.1
62.6	38.94	35.08	37.01	3.86
61.8	30.31	30.37	30.34	0.06
61	29.89	30.05	29.97	0.16

(g) Ct Value of *FAP* Primer Annealing Temperature Optimization

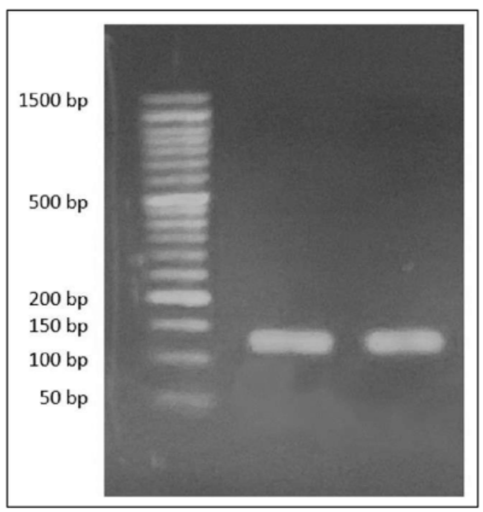

(h) Electrophoresis Validation on Product Length of *FAP* Primer

Figure 4. Experiment Validation using qPCR and Electrophoresis for *FAP* Primer. Results from qPCR run showed (a) successful amplification process, (b) specific dissociation of amplicons, (c) specific melt peak of amplicons, with no primer-dimer evident based on (d) no amplification, (e) no dissociation and (f) no melt peak from NTC reaction, (g) temperature gradient qPCR run showed the optimum annealing temperature with lowest Ct detected, (h) electrophoresis run showed specific amplicon with targeted length.

6h). This implied that the amplicon length corresponds to the designed primer product length of 123 bp. The NTC analysis showed that there was no possibility of primer-dimer and hairpin formation based on amplification (Figure 6d), melt curve (Figure 6e), and melt peak (Figure 6f) charts.

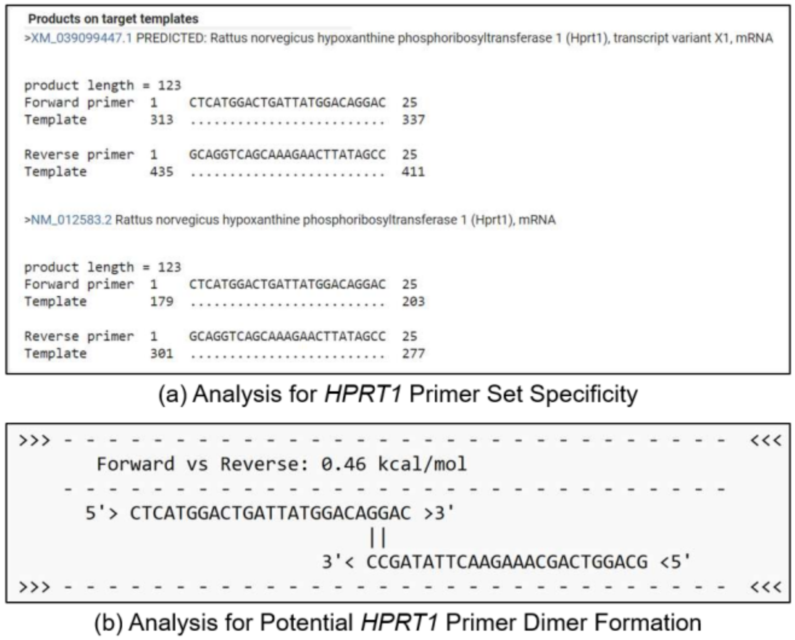

Figure 5. Bioinformatic Primer Analysis Results for *HPRT1* Primer. (a) Analysis result from Primer-Blast (https://www.ncbi.nlm.nih.gov/tools/primer-blast/) showed primer specificity to *HPRT1* mRNA. (b) Analysis result from PrimerDimer (http://www.primer-dimer.com/) showed low indication of Primer Dimer Formation with two hydrogen bonds.

PDGFB Primer

The suitable *PDGFB* primer was from Lee et al. (2016) with 5'- ACCACTCCATCCGCTCCTTT-3' for forward primer and 5'-TGTGCTCGGGTCATGTTCAA-3' for reverse primer. The calculated melting temperature was 63.22°C for forward primer and 63.69°C for a reverse primer with a 0.47°C difference. The GC contents for both primers were 55 and 50% respectively. The primer pair can be said to be specific with no unintended possible amplification (Figure 7a). The primer pair was possibly two hydrogen bonds at the 3' end of forward and reverse primer (Figure 7b). The hairpin formation possibility for both forward and reverse primer was none. The primer pair alignment with similar sequences from Nucleotide Blast resulted in 100 bp amplicon.

The amplification chart (Figure 8a) showed that the primer pair could prime the amplification of the cDNA template resulting in specific dissociation (Figure 8b) and one peak of melt peak chart (Figure 8c). The Ct values indicated that the optimal annealing temperature was 62.6°C (Figure 8g). The specific targeting of primer was validated with one visualization in electrophoresis, parallel to 100 bp marker band (Figure 8h). The NTC results from the amplification plot (Figure 8d), melt curve (Figure 8e), and melt peak (Figure 8f) charts showed that there was no possibility of primer-dimer and hairpin formation.

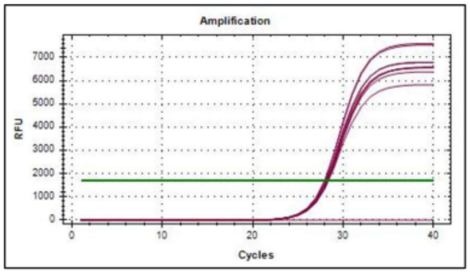

(a) Amplification Plot of *HPRT1* Primer Annealing Temperature Optimization

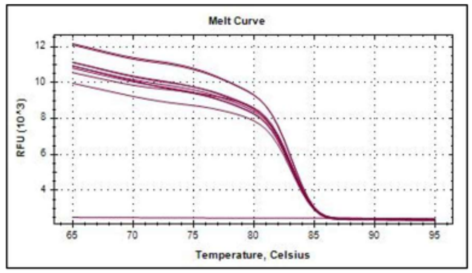

(b) Melt Curve of *HPRT1* Primer Annealing Temperature Optimization

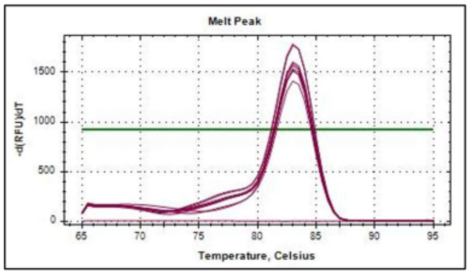

(c) Melt Peak of *HPRT1* Primer Annealing Temperature Optimization

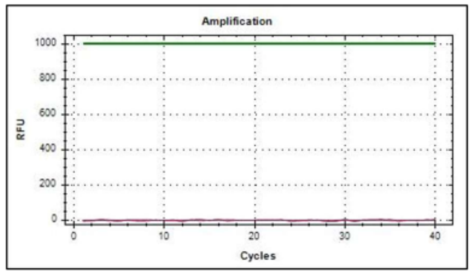

(d) Amplification Plot of *HPRT1* Primer NTC

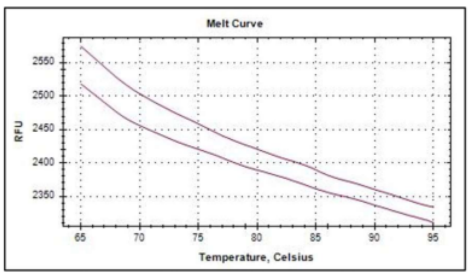

(e) Melt Curve of *HPRT1* Primer NTC

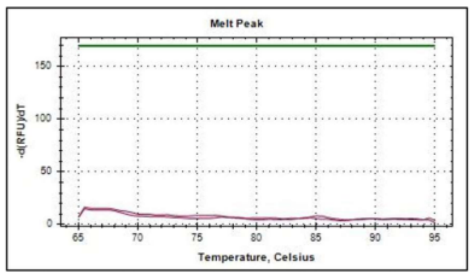

(f) Melt Peak of *HPRT1* Primer NTC

HPRT1				
Temperature (°C)	Ct1	Ct2	Ct Average	Ct Difference
64.8	28.36	28.3	28.33	0.06
63.6	28.28	28.28	28.28	0
62.6	27.97	27.95	27.96	0.02
61.8	28.16			
61	28.15	28.09	28.12	0.06

(g) Ct Value of *HPRT1* Primer Annealing Temperature Optimization

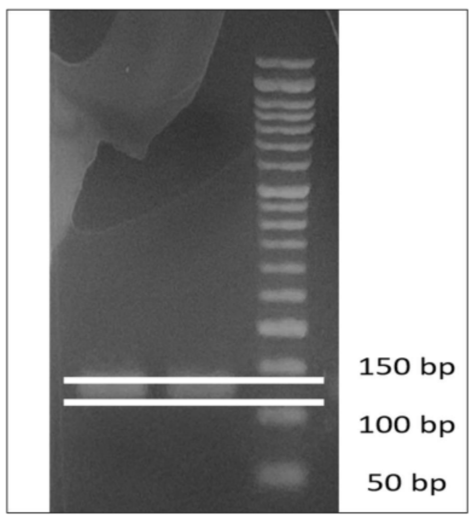

(h) Electrophoresis Validation on Product Length of *HPRT1* Primer

Figure 6. Experiment Validation using qPCR and Electrophoresis for *HPRT1* Primer. Results from qPCR run showed (a) successful amplification process, (b) specific dissociation of amplicons, (c) specific melt peak of amplicons, with no primer-dimer evident based on (d) no amplification, (e) no dissociation and (f) no melt peak from NTC reaction, (g) temperature gradient qPCR run showed the optimum annealing temperature with lowest Ct detected, (h) electrophoresis run showed specific amplicon with targeted length.

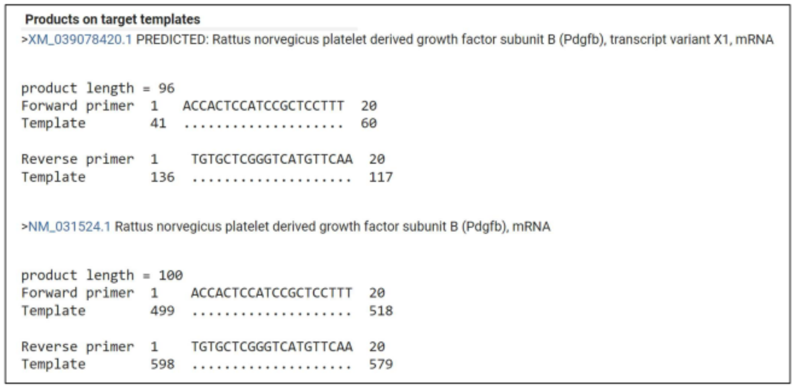

(a) Analysis for *PDGFB* Primer Set Specificity

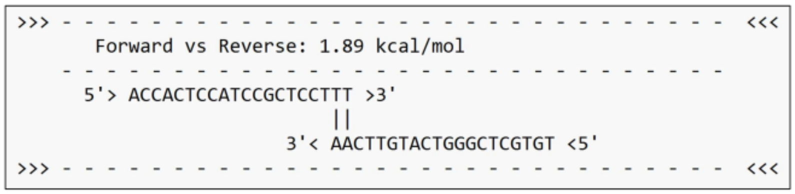

(b) Analysis for Potential *PDGFB* Primer Dimer Formation

Figure 7. Bioinformatic Primer Analysis Results for *PDGFB* Primer. (a) Analysis results from Primer-Blast (https://www.ncbi.nlm.nih.gov/tools/primer-blast/) showed primer specificity to *PDGFB* mRNA. (b) Analysis result from PrimerDimer (http://www.primer-dimer.com/) showed low indication of Primer Dimer Formation with two hydrogen bonds.

PIK3R1 Primer

A suitable *PIK3R1* primer was found in an article from Cai et al. (2019). The primer sequences were 5'- CGAAAACACAGAAGACCAATACTCA -3' for forward primer and 5'- TCCCTCGCAATAGGTTCTCG-3' for reverse primer. The calculated melting temperatures were 61.71°C for forward primer and 62.54°C for a reverse primer with a 0.83°C difference. The GC contents were 40% for forward primer and 55% for reverse primer. The Primer Blast result showed that this primer pair was specific to its target gene (Figure 9a). The possibility of primer dimer formation could occur on the 3' end of reverse primers with two hydrogen bonds (Figure 9b). The hairpin formation possibility was not possible for each primer. The alignment of the primer pair with a similar sequence showed that the primer produces 122 bp amplicon.

The amplification chart showed that the primer pair was able to prime the qPCR amplification (Figure 10a) with one possible specific amplicon due to one specific dissociation (Figure 10b) and one melt peak (Figure 10c) produced. The optimal temperature was 62.6°C as the lowest Ct value was from 62.6°C annealing temperature (Figure 10g). The electrophoresis result showed that the amplicon was in between the 100 and 150 bp suggesting that the amplicon has the targeted amplicon length of 122 bp (Figure 10h). The NTC analysis showed that there was no possibility of primer-dimer and hairpin formation based on amplification plot (Figure 10d), melt curve (Figure 10e), and melt peak (Figure 10f) charts.

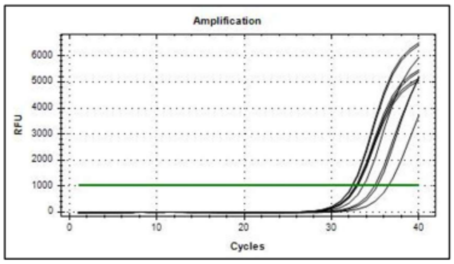

(a) Amplification Plot of *PDGFB* Primer Annealing Temperature Optimization

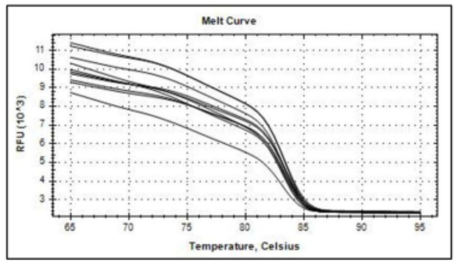

(b) Melt Curve of *PDGFB* Primer Annealing Temperature Optimization

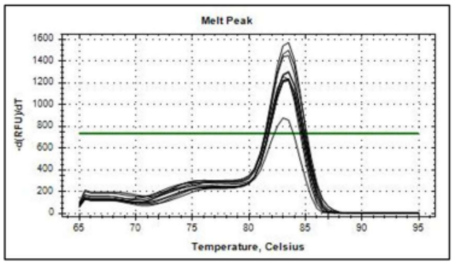

(c) Melt Peak of *PDGFB* Primer Annealing Temperature Optimization

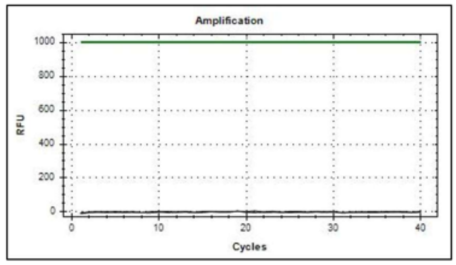

(d) Amplification Plot of *PDGFB* Primer NTC

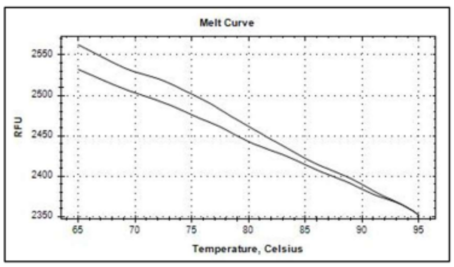

(e) Melt Curve of *PDGFB* Primer NTC

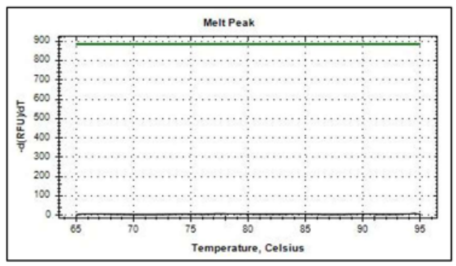

(f) Melt Peak of *PDGFB* Primer NTC

PDGFB				
Temperature (°C)	Ct1	Ct2	Ct Average	Ct Difference
64.8	36.53	34.99	35.76	1.54
63.6	35.25	33.66	34.455	1.59
62.6	32.45	32.37	32.41	0.08
61.8	32.85	33.02	32.935	0.17
61	32.84	33.02	32.93	0.18

(g) Ct Value of *PDGFB* Primer Annealing Temperature Optimization

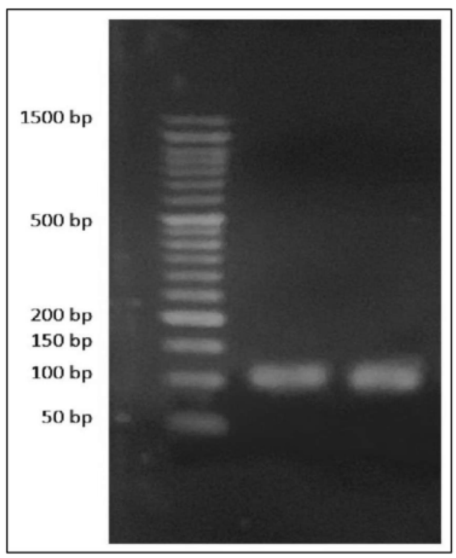

(h) Electrophoresis Validation on Product Length of *PDGFB* Primer

Figure 8. Experiment Validation using qPCR and Electrophoresis for *PDGFB* Primer. Results from qPCR run showed (a) successful amplification process, (b) specific dissociation of amplicons, (c) specific melt peak of amplicons, with no primer-dimer evident based on (d) no amplification, (e) no dissociation and (f) no melt peak from NTC reaction, (g) temperature gradient qPCR run showed the optimum annealing temperature with lowest Ct detected, (h) electrophoresis run showed specific amplicon with targeted length.

```
Products on target templates
>NM_013005.2 Rattus norvegicus phosphoinositide-3-kinase regulatory subunit 1 (Pik3r1), mRNA

product length = 122
Forward primer  1     CGAAAACACAGAAGACCAATACTCA  25
Template        2373  .........................  2397

Reverse primer  1     TCCCTCGCAATAGGTTCTCG  20
Template        2494  ....................  2475

>XM_008760659.3 PREDICTED: Rattus norvegicus phosphoinositide-3-kinase regulatory subunit 1 (Pik3r1), transcript variant X3, mRNA

product length = 122
Forward primer  1     CGAAAACACAGAAGACCAATACTCA  25
Template        2819  .........................  2843

Reverse primer  1     TCCCTCGCAATAGGTTCTCG  20
Template        2940  ....................  2921

>XM_006231868.4 PREDICTED: Rattus norvegicus phosphoinositide-3-kinase regulatory subunit 1 (Pik3r1), transcript variant X2, mRNA

product length = 122
Forward primer  1     CGAAAACACAGAAGACCAATACTCA  25
Template        1927  .........................  1951

Reverse primer  1     TCCCTCGCAATAGGTTCTCG  20
Template        2048  ....................  2029
```

(a) Analysis for *PIK3R1* Primer Set Specificity

```
>>> - - - - - - - - - - - - - - - - - - - - - - - - - - - - - - -  <<<
      Reverse vs Reverse: -3.64 kcal/mol
    - - - - - - - - - - - - - - - - - - - - - - - - - - - - - - -
     5'> TCCCTCGCAATAGGTTCTCG >3'
                          ||
                     3'< GCTCTTGGATAACGCTCCCT <5'
>>> - - - - - - - - - - - - - - - - - - - - - - - - - - - - - - -  <<<
```

(b) Analysis for Potential *PIK3R1* Primer Dimer Formation

Figure 9. Bioinformatic Primer Analysis Results for *PIK3R1* Primer (a) Analysis result from Primer-Blast (https://www.ncbi.nlm.nih.gov/tools/primer-blast/) showed primer specificity to *PIK3r1* mRNA. (b) Analysis result from PrimerDimer (http://www.primer-dimer.com/) showed low indication of Primer Dimer Formation with two hydrogen bonds.

VCAM1 Primer

Fasta sequence of NM_012889.2 was used for the *VCAM1* primer design template. One set of the resulting primers was 5'-TTGGGGATTCCGTTGTTCTG-3' for forward primer and 5'-TGTAGCCCCTTCATCCCTCA-3' for reverse primer. The calculated melting temperatures were 63.10°C for forward primer and 62.86°C for a reverse primer with a 0.24°C difference. The GC contents were 50% for forward primer and 55% for reverse primer. It was then analyzed for gene specificity, resulting in specific targeted to desired *VCAM1* mRNA sequence. This primer set 116 bp amplicon without showing the possibility of unintended priming site on other genes in the same sample animal (Figure 11a). The primer dimer analysis showed a possibility of primer dimer at the end of primers with two hydrogen bonds (Figure 11b). The primer hairpin analysis showed that both forward and reverse primers had no possibilities for primer hairpin formation. The identical sequence was then aligned showing that the forward primer and reverse primer confine amplification to produce 116 bp amplicon.

The amplification chart showed that the primer pair could amplify the cDNA samples (Figure 12a). The melt curve chart showed one specific dissociation (Figure 12b) and the melting peak showed one peak (Figure 12c) indicating one amplicon being amplified. The lowest average Ct value was using 61°C but with 0.88°C difference being the highest. The annealing temperature resulted in the slightly higher Cq and the

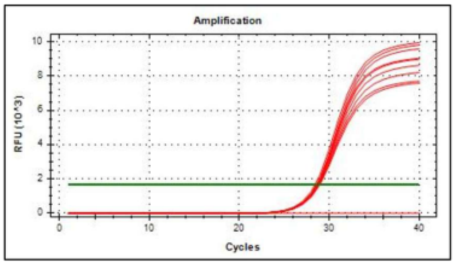

(a) Amplification Plot of *PIK3R1* Primer Annealing Temperature Optimization

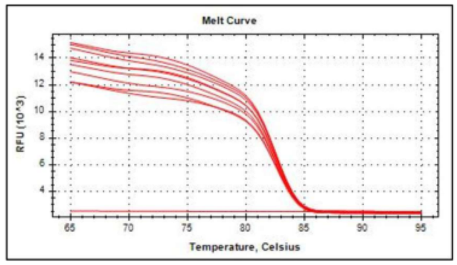

(b) Melt Curve of *PIK3R1* Primer Annealing Temperature Optimization

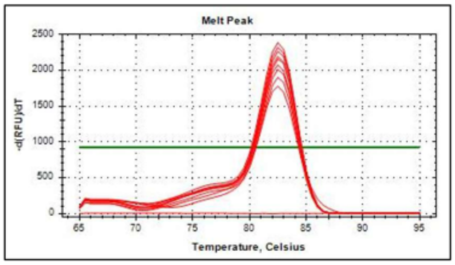

(c) Melt Peak of *PIK3R1* Primer Annealing Temperature Optimization

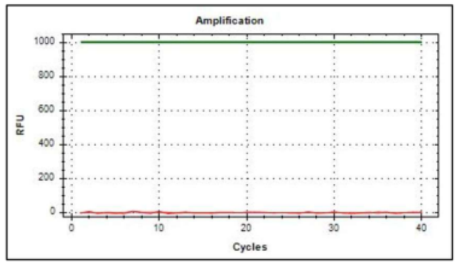

(d) Amplification Plot of *PIK3R1* Primer NTC

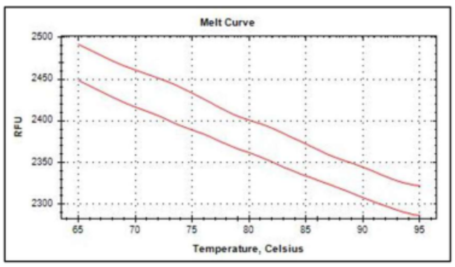

(e) Melt Curve of *PIK3R1* Primer NTC

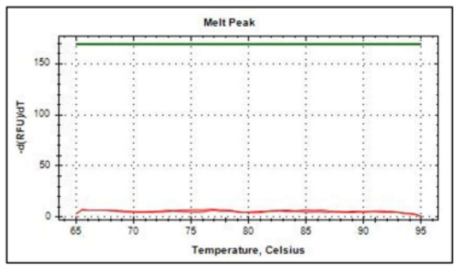

(f) Melt Peak of *PIK3R1* Primer NTC

PIK3R1				
Temperature (°C)	Ct1	Ct2	Ct Average	Ct Difference
64.8	28.98	28.84	28.91	0.14
63.6	28.88	28.76	28.82	0.12
62.6	28.69	28.41	28.55	0.28
61.8	28.72	28.58	28.65	0.14
61		28.59		

(g) Value of *PIK3R1* Primer Annealing Temperature Optimization

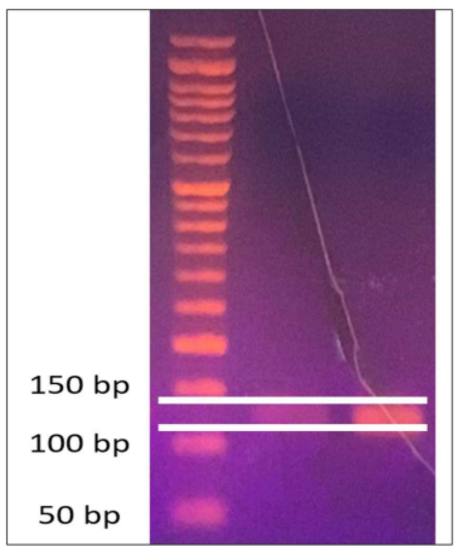

(h) Electrophoresis Validation on Product Length of *PIK3R1* Primer

Figure 10. Experiment Validation using qPCR and Electrophoresis for *PIK3R1* Primer. Results from qPCR run showed (a) successful amplification process, (b) specific dissociation of amplicons, (c) specific melt peak of amplicons, with no primer-dimer evident based on (d) no amplification, (e) no dissociation and (f) no melt peak from NTC reaction, (g) temperature gradient qPCR run showed the optimum annealing temperature with lowest Ct detected, (h) electrophoresis run showed specific amplicon with targeted length.

lower difference was 61.8°C (Figure 12g). Based on melt peak and electrophoresis, the analysis showed one band between 100 and 150 bp corresponding to predicted amplicon length (Figure 12h). The NTC results showed that there was no indication of primer-dimer and hairpin formation based on amplification plot (Figure 12d), melt curve (Figure 12e), and melt peak (Figure 12f) charts.

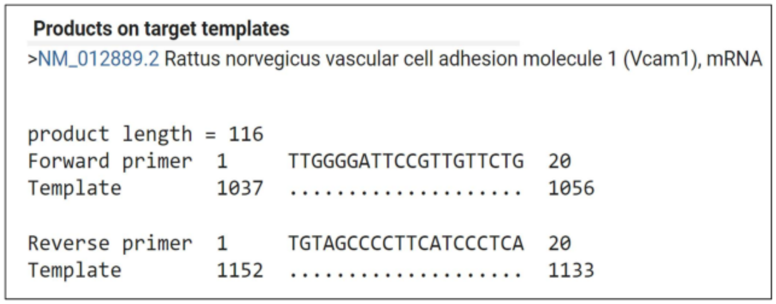

(a) Analysis for *VCAM1* Primer Set Specificity

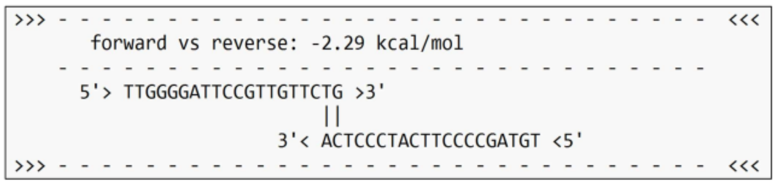

(b) Analysis for Potential *VCAM1* Primer Dimer Formation

Figure 11. Bioinformatic Primer Analysis Results for *VCAM1* Primer. (a) Analysis result from Primer-Blast showed primer specificity to *VCAM1* mRNA (https://www.ncbi.nlm.nih.gov/tools/primer-blast/). (b) Analysis result from PrimerDimer (http://www.primer-dimer.com/) showed low indication of Primer Dimer Formation with two hydrogen bonds.

Discussion

Here we reported the qPCR primer sequence and validation approach for *ACTA2*, *FAP*, *HPRT1*, *PDGFB*, *PIK3R1*, and *VCAM1* for the reagent condition of SYBR Green I and 3 mM $MgCl_2$. This study provided evidence of bioinformatic analytical approach, experimental validation, and tested qPCR primer set for published primer pairs (*HPRT1*, *PDGFB*, and *PIK3R1*) and newly designed genes (*ACTA2*, *FAP*, and *VCAM1*). SYBR Green I can be reliably used in relative quantitative if primers are properly constructed (Ferreira et al. 2006). $MgCl_2$ can affect the primer priming process. Thus, we made an *in-silico* attempt to predict suitable primer and laboratory work for validation. The bioinformatic analysis results suggested sequences with the highest possibility and suitability. The laboratory experimental validation results indicated that the analyzed primer quality in functioning and suitability with qPCR reagent and reaction condition is quite adequate.

The factors accounted for in this in silico analysis were: a) primer melting temperature; b) Tm difference between forward and reverse primer; c) primer GC content; d) primer specificity; e) Hairpin possibility; and f) Dimer formation possibility. Based on the reagent requirement, primer Tm was determined to be within the range of 60-65°C Tm. The comparison was made against the database. The least suitable primer pairs were eliminated (data is not shown). The value of melting temperature was used as the annealing temperature as stated by the manufacture protocol.

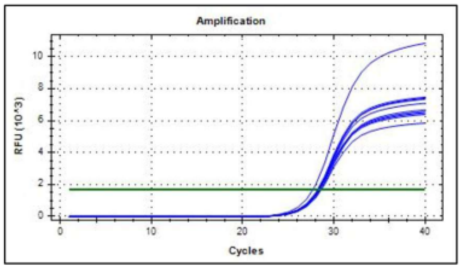

(a) Amplification Plot of *VCAM1* Primer Annealing Temperature Optimization

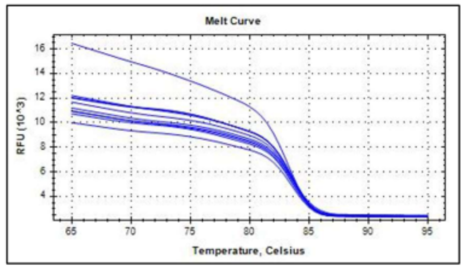

(b) Melt Curve of *VCAM1* Primer Annealing Temperature Optimization

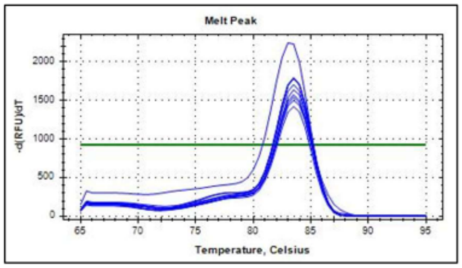

(c) Melt Peak of *VCAM1* Primer Annealing Temperature Optimization

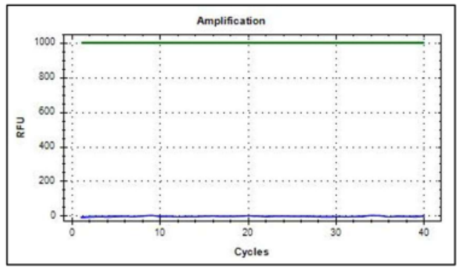

(d) Amplification Plot of *VCAM!* Primer NTC

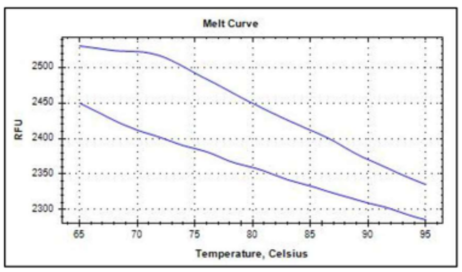

(e) Melt Curve of *VCAM1* Primer NTC

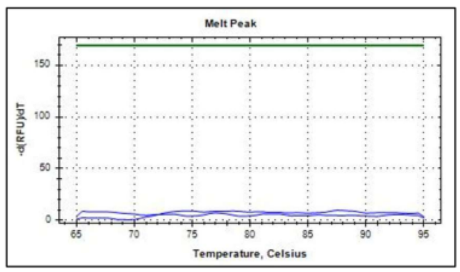

(f) Melt Peak of *VCAM1* Primer NTC

VCAM1				
Temperature (°C)	Ct1	Ct2	Ct Average	Ct Difference
64.8	28.4	28.28	28.34	0.12
63.6	28.59	28.39	28.49	0.2
62.6	28.24	28.31	28.275	0.07
61.8	28.33	28.2	28.265	0.13
61	27.67	28.55	28.11	0.88

(g) Ct Value of *VCAM1* Primer Annealing Temperature Optimization

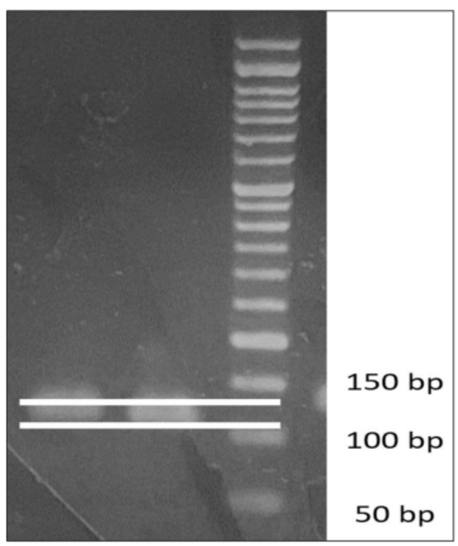

(h) Electrophoresis Validation on Product Length of *VCAM1* Primer

Figure 12. Experiment Validation using qPCR and Electrophoresis for *VCAM1* Primer. Results from qPCR run showed (a) successful amplification process, (b) specific dissociation of amplicons, (c) specific melt peak of amplicons, with no primer-dimer evident based on (d) no amplification, (e) no dissociation and (f) no melt peak from NTC reaction, (g) temperature gradient qPCR run showed the lower optimum annealing temperature, (h) electrophoresis run showed specific amplicon with targeted length.

The technical run of every qPCR reaction follows the manufacture protocol that specifies the temperature of cycling steps such as pre-denaturation, denaturation, and extension, except for annealing temperature. Primer melting temperature was determined within the range of 60 -65°C based on reagent requirement. The melting temperature was used as annealing temperature as stated by the manufacturer. According to (Fittipaldi et al. 2010), a high annealing temperature is advantageous in facilitating the dye-binding specificity with DNA. This evades both reaction inhibition of PCR and the formation of primer dimer. As the consideration of using melting temperature as annealing temperature, optimal primer melting temperature was set to the median of the suggested annealing temperature range. This was based on the consideration of statistical normal distribution. The resulting analyzed melting temperature used as annealing temperature was between 61.71-63.69°C. These temperatures were in corresponded to GC content. Primer GC content was chosen to be 40-50% to ensure the strength of the annealing mechanism between primer and template. This is because the hydrogen bond between GC is more stable than AT (Ouldridge et al. 2013).

The melting temperature difference was chosen to have a maximum of 1°C difference in facilitating a parallel annealing starting point. This can maximize two amplicons to be produced by the end of each cycle as the annealing process occurs simultaneously. The small melting temperature difference in annealing temperature aims to avoid unintended primer annealing in each cycle (Hashish et al. 2021). The analyzed melting temperature differences ranged from 0.03 to 0.84°C.

Primer Blast was used to screen the specificity of pre-existing (both from published articles and newly designed) primers against the gene database. Primer specificity was selected to eliminate the possibility of quantifying the wrong amplicon target. Mispriming could occur due to homologous regions and random mismatches, resulting in amplification of non-intended targets (Ye et al. 2012). The specificity screening results showed no indication of mispriming at homologous regions and arbitrary mismatch. Thus, the primer sequences were expected to be specific to the genes of interest.

Primer dimer and hairpin formation possibility was used in selecting the least possible formation and eliminating the greater possible formation present. In all the above dimer formation possibility analysis attempts, the least dimer possibility was that two hydrogen bonds occurred at the 3' primer sequence. Thornton & Basu (2011) stated that primer dimer with 3' complementary matches more than two base pairs should be avoided. The primer pairs in this article have the least complementary possible formation of two bp. With numerous attempts to find the least possible dimer formation, all the primer sequences showed the least possible dimer formation corresponding to the previous statement. Hairpin formation can also affect amplification. This is due to their loop size and complementarity in the 3' end. The formation of loop and complementarity may elevate the possibility of self-complementary amplification. This can result in declining amplification efficiency (Singh et al. 2000). Each of the primer pair sets showed no indication of hairpin formation.

The alignment approach was done to address primer localization and ensuring the amplicon length. The alignment result confirmed the specificity of amplicon length and localization. The adequate possible primer localization site is on the conserved regions. This is due to the possibility of the high level of variation found in the sequence may elevate the degenerate site thus increasing the potential of primer-dimer (Brodin et al. 2013).

Laboratory experimental validation covered amplification chart, melt curve chart, melt peak chart, Cq value of annealing temperature optimization, amplicon visualization band on electrophoresis, and NTC analysis. The amplification charts showed that primer could prime amplification. Melt curve and melt peak charts showed the specificity of the amplicon, with no detection of amplicon at a lower temperature. Electrophoresis validation results indicated that the amplicon was the targeting amplicon based on the amplicon visualization band. The NTC result showed no possibility of primer-dimer and hairpin formation which validates the melt curves with no peak at a lower temperature. The qPCR showed good specification due to one dissociation peak on the melt peak curve and one visualization band on electrophoresis. This indicates that using this sequence (and potentially any type of sequence) was suitable with the chemical reagent specifically SYBR Green I fluorophore and three mM of $MgCl_2$. In addition, to ensure qPCR primer before use in gene expression analysis, NTC reaction was tested to see the possible formation of hairpin and primer dimer. All data from each primer pair shows no indication of either hairpin or primer dimer formation.

The amplification chart showed the amplification curve based on exponential fluorescence emission. The results from all primer pair sets showed that the primers could proceed with the priming process, leading to the amplification of templates. Thus, the generated fluorescence emission in an exponential manner is the outcome of the exponential amplification of primer priming in the chain reaction (Goda et al. 2015).

The annealing temperature results varied in variable temperature points. This is due to various factors. Aside from the fact that annealing temperature is dependent on primer sequence (inherent properties), the annealing temperature must be in the range of the efficient temperature range of chemical reagent mode of work, including the suitability to SYBR Green I reagent with buffer including $MgCl_2$. The reagent used in this approach was Bioline SYBR Green I. Thus, it is an important approach to closely look at the annealing temperature required by the manufacture. Thornton & Basu (2011) explained that primer GC content has a control on the melting temperature of primer. The annealing temperature is usually 3 to 5°C above the melting temperature.

Aside from the GC-controlled annealing temperature of primer, the qPCR reaction may be affected by the mode of action of SYBR Green I. There is an optimal temperature for SYBR. Thornton & Basu (2011) specifically mentioned that optimal qPCR primer melting temperature using SYBR Green fluorophore was between 62 and 67°C, with an optimal melting temperature of 63°C. This is correlated with the bioinformatically analyzed primer melting temperature and the instruction of manufacture (Bioline). The optimal temperature for each primer pair set was determined based on the lowest Cq value obtained across the annealing temperature range (Gaby & Buckley 2017). The results showed that the *ACTA2* and *FAP* had the most suitable annealing temperature of 61°C. The primer pair sets of *HPRT1*, *PDGFB*, and *PIK3R1* had the most suitable annealing temperature of 62.6°C. Meanwhile, *VCAM1* primer pair set had the most considerable annealing temperature of 61.6°C. The validation of temperature covering annealing temperature of 61-65°C showed that optimal annealing temperatures were below the calculated melting temperature. The results suggest that the optimal annealing temperature is inconsistent with the inherent GC content factor in the primer. This is due to the evidence that the higher the GC content of the primers, the lower the annealing temperatures were and vice versa. The results showed that it is more likely that the higher melting temperature differences are coherent with the higher suitable validated annealing temperature. Although this evaluation has not been explored further, the cause of this phenomenon remains unclear.

A melt curve was also run as suggested by (Thornton & Basu 2011) for the purpose of detecting secondary products for taking thoughtful conclusions. As stated by (Gregory et al. 2012), dissociation curves were used to analyze a single amplicon generated in each run by each primer pair. The increase in temperature leads to the denaturation of amplicon, resulting in single-stranded DNA. This occurrence gives rise to fluorophore dissociation, causing the fluorescence emission to plummet (Ahmed et al. 2017). The results showed one descending fluorescence in the melt curve of each amplification of each primer pair set. This excludes the *FAP* amplicon melt curve with the additional descending fluorescence in the lower annealing temperature.

The primer pairs indicatedspecificity based on the melt charts showing one peak. Based on a preliminary experiment by Ririe et al. (1997), melting peak count correlates with electrophoresis results. This is due to the dissociation of PCR products with the accounted factor of GC ratio, length, and sequence. Melt peak analysis delivers higher certainty referring to the fluorescence obtained during qPCR acquired from the targeted product (Ririe et al. 1997). The melt curve profile was then plotted in the negative derivative of fluorescence vs temperature. This represents the peak at which the dissociation event occurs (Vulchi et al. 2021). Corresponding to melt curve results, the melting peak from every single primer pair was one specific melt peak excluding the melting peak for the *FAP* primer pair set with additional lower annealing temperature melt peak.

Gel electrophoresis was done for amplicon identity validation. One band in electrophoresis indicates one type of amplicon. This is because the generation of one band is caused by the same amplicon length with the same molecular weight (Ririe et al. 1997). The results showed that the amplicon generated from each primer pair set of the most suitable annealing temperature has the corresponding product length as bioinformatic analysis. It suggests that the amplicon is specific and the primer pair sets were able to prime specified regions representing the targeted cDNA.

There are two purposes of no template control (NTC) reaction analysis: to assess a) the presence of contamination in the reaction solution (cross-contamination during reaction setup stated by (Su et al. 2020)) and b) primer-dimer formation (Taylor et al. 2010; D'haene et al. 2010). In this case, the NTC was used to check the primer-dimer formation possibility before gene expression qPCR analysis. This is important for ensuring primer quality and minimizing unexpected bias due to primer-dimer. A melt curve was also run as suggested by Thornton & Basu (2011) to detect secondary products. In testing primer quality control, an NTC reaction was generated by replacing the template with molecular grade water (Alonso et al. 2018). These NTCs experiments were done as stated in Taylor et al. (2010), with two technical replicate reactions.

In the possibility of primer dimer formation, the formation may be detected in qPCR NTC reaction (Morinha et al. 2020) by no Cq value being detected (Cheung et al. 2021). Although no amplicon detected in NTC, if the presence of an additional melt peak detected from the melt curve, it means nonspecific products are being amplified (Thornton & Basu 2011). All data from NTC reactions of each primer pair set shows no indication of either hairpin or primer dimer. This is based on the results of the amplification plot, melt curve, and melt peak charts. These results correspond to bioinformatic analysis of primer-dimer and primer hairpin formation possibilities with no noteworthy indication of hairpin formation.

Double-strand DNA can be detected using SYBR Green I. This molecule can bind to double-strand DNA. Once it is intercalated to dsDNA, the fluorescence occurrs to be detected. When single-strand DNA is present, weaker fluorescence occurs at 520 nm (Wang et al. 2019). When double-strand DNA is present, the stronger fluoresence is emitted. The previous study showed that the fluorescence intensity change is close to the chromophore lifetime change. That finding explains the SYBR Green I quenching dynamic in solution. It is important to underline that the function of fluorescence decay is sensitively impacted by the distribution of chromophore molecule conformers, reflecting the presence of different types of interactions with other molecules (Dragan et al. 2012).

With the storing condition of SYBR (mentioned below), this article ensures the quality of SYBR Green I used. The SYBR Green I reagent was stored in a plastic-based storage. This storing system was considered because plastic-based storage does not adsorb SYBR Green I, thus maintaining fluorescence ability. The SYBR Green I stock solution is also stored in a plastic tube enclosed with foil wrapping as light protection. The storage condition used for SYBR Green I was in –20°C which ensures its stability during storage (Bourzac et al. 2003). Thus, the results may be convinced to be reliable because the SYBR Green I and $MgCl_2$ condition are ensured to be reliable with the maintained conditions.

$MgCl_2$ concentration contained in the mix, as stated in Bioline Manufacture's protocol was 3 mM. Thornton & Basu (2011) explained that GC content has a control on the melting temperature of primer. The annealing temperature is usually 3 to 5°C above the melting temperature. In the practical run, specific salt buffer and $MgCl_2$ concentration can modify primer melting temperature. $MgCl_2$ can stabilize nucleic acid duplex stability (Nakano et al. 1999). Primer melting temperature can be affected by Mg^{2+} associated with primer GC content (Von Ahsen et al. 2001). The reality that reagents are offered varies with the additional consideration of various unique buffer content ratios. It may alter the $MgCl_2$ optimal concentration and annealing temperature required (Tajima et al. 2001).

The bioinformatics prediction and experimental validation evidences showed the primer pair sets were suitable with SYBR Green I and three mM of $MgCl_2$. This might indicate that these sequences can be used for the following analysis. This can be done especially with the chemical reagent of SYBR Green I with three mM of $MgCl_2$, in ensuring the priming of amplification process. The explained procedures also could be used for qPCR primer bioinformatic prediction and validation assessment approach. This is beneficial when the optimum temperatures of SYBR Green I and qPCR primer sequences are considered.
minima veniam, quis nostrum exercitationem ullam corporis suscipit laboriosam, nisi ut aliquid ex ea commodi consequatur? Quis autem vel eum iure reprehenderit qui in ea voluptate velit esse quam nihil molestiae consequatur.

CONCLUSION

The primer pair sequences for *ACTA2*, *FAP*, *HPRT1*, *PDGFB*, *PIK3R1*, and *VCAM1* stated above have been analyzed to produce a suitable amplicon for qPCR using *Rattus norvegicus* cDNA with SYBR Green I, annealing temperature range of 60-65°C with three mM $MgCl_2$ and this approach can be useful for consideration in qPCR primer preparation.

AUTHORS CONTRIBUTION

G.P. contributed in methodology, collected and analyzed the data and wrote the manuscript, N.A. and F.A. conceived the conceptualization of experimental design and methodology, R.P. supervised all the process.

ACKNOWLEDGMENTS

We would like to thank Endah Sri Palupi, Retno Wahidah and Daniel Saputra Wahyudi for providing help in the cDNA sample preparation.

CONFLICT OF INTEREST

The authors declare that there is no conflict of interest.

REFERENCES

Ahmed, F.E. et al., 2017. Role of Melt Curve Analysis in Interpretation of Nutrigenomics' MicroRNA Expression Data. *Cancer Genomics and Proteomics*, 14(6), pp.469–481. doi: 10.21873/cgp.20057.

Alonso, G.C. et al., 2018. A Quest to Find Good Primers for Gene Expression Analysis of Candida albicans from Clinical Samples. *Journal of Microbiological Methods*, 147, pp.1–13. doi: 10.1016/j.mimet.2018.02.010.

Bourzac, K.M., LaVine, L.J. & Rice, M., 2003. Analysis of DAPI and SYBR Green I as Alternatives to Ethidium Bromide for Nucleic Acid Staining in Agarose Gel Electrophoresis. *Journal of Chemical Education*, 80(11), pp.1292–1296. doi: 10.1021/ed080p1292.

Brodin, J. et al., 2013. A Multiple-Alignment based Primer Design Algorithm for Genetically Highly Variable DNA Targets. *BMC Bioinformatics*, 14, 255. doi: 10.1186/1471-2105-14-255.

Brown, J.R. et al., 2021. Comparison of SARS-CoV-2 N Gene Real-time RT-PCR Targets and Commercially Available Mastermixes. *Journal of Virological Methods*, 295, 114215. doi: 10.1016/j.jviromet.2021.114215.

Cai, W. et al., 2019. MicroRNA-24 Attenuates Vascular Remodeling in Diabetic Rats through PI3K/Akt Signaling Pathway. *Nutrition, Metabolism and Cardiovascular Diseases*, 29(6), pp.621–632. doi: 10.1016/j.numecd.2019.03.002.

Camorani, S., Hill, B.S. & Fontanella, R., et al. 2017. Inhibition of BM-MSCs Homing Towards TNBC Microenvironment Using an Anti-PDGFRβ Aptamer. *Theranostics*, 7(14), pp.3595–3607

Canh, V.D. et al., 2020. Application of Capsid Integrity (RT-)qPCR to Assessing Occurrence of Intact Viruses in Surface Water and Tap Water in Japan. *Water Research*, 189, 116674. doi: 10.1016/j.watres.2020.116674.

Caselli, E. et al., 2021. Looking for More Reliable Biomarkers in Breast Cancer: Comparison Between Routine Methods and RT-qPCR. *PLoS ONE*, 16(9), e0255580. doi: 10.1371/journal.pone.0255580.

Cheung, H.W. et al., 2021. A Duplex qPCR Assay for Human Erythropoietin (EPO) Transgene to Control Gene Doping in Horses. *Drug Testing and Analysis*, 13(1), pp.113–121. doi: 10.1002/dta.2907.

Costa, A. et al., 2018. Fibroblast Heterogeneity and Immunosuppressive Environment in Human BC. *Cancer Cell*, 33(3), pp.463-479.e10.

Covey, S.D., 2021. An Adaptable Dry Lab for SYBR Based RT-qPCR Primer Design to Reinforce Concepts in Molecular Biology and Nucleic Acids. *Biochemistry and Molecular Biology Education*, 49(2), pp.262–270. doi: 10.1002/bmb.21446.

Cuevas-Ferrando, E. et al., 2021. Platinum Chloride-based Viability RT-qPCR for SARS-CoV-2 Detection in Complex Samples. *Scientific Reports*, 11, 18120. doi: 10.1038/s41598-021-97700-x.

D'haene, B., Vandesompele, J. & Hellemans, J., 2010. Accurate and Objective Copy Number Profiling using Real-Time Quantitative PCR. *Methods*, 50(4), pp.262–270. doi: 10.1016/j.ymeth.2009.12.007.

Dragan, A.I. et al., 2012. SYBR Green I: Fluorescence Properties and Interaction with DNA. *Journal of Fluorescence*, 22(4), pp.1189–1199. doi: 10.1007/s10895-012-1059-8.

Ferreira, I.D., do Rosario, V.E. & Cravo, P.V.L., 2006. Real-time Quantitative PCR with SYBR Green I Detection for Estimating Copy Numbers of Nine Drug Resistance Candidate Genes in Plasmodium falciparum. *Malaria Journal*, 5(1). doi: 10.1186/1475-2875-5-1.

Fiechter, R.H. et al., 2021. IL-12p40/IL-23p40 Blockade with Ustekinumab Decreases the Synovial Inflammatory Infiltrate through Modulation of Multiple Signaling Pathways Including MAPK-ERK and Wnt. *Frontiers in Immunology*, 12, 611656. doi: 10.3389/fimmu.2021.611656.

Fittipaldi, M., Codony, F. & Morato, J., 2010. Comparison of Conventional Culture and Real-Time Quantitative PCR using SYBR Green for Detection of Legionella pneumophila in Water Samples. *African Journals Online*, 36(4), pp.417–424. doi: 10.4314/wsa.v36i4.58411.

Gaby, J.C. & Buckley, D.H., 2017. The Use of Degenerate Primers in qPCR Analysis of Functional Genes Can Cause Dramatic Quantification Bias as Revealed by Investigation of nifH Primer Performance. *Microbial Ecology*, 74(3), pp.701–708. doi: 10.1007/s00248-017-0968-0.

Goda, T., Tabata, M. & Miyahara, Y., 2015. Electrical and Electrochemical Monitoring of Nucleic Acid Amplification. *Frontiers in Bioengineering and Biotechnology*, 3(29). doi: 10.3389/fbioe.2015.00029.

Gregory, S.M. et al., 2012. Latent Kaposi's Sarcoma-Associated Herpesvirus Infection of Monocytes Downregulates Expression of Adaptive Immune Response Costimulatory Receptors and Proinflammatory Cytokines. *Journal of Virology*, 86(7), pp.3916–3923. doi: 10.1128/jvi.06437-11.

Hargreaves, S.K., Roberto, A.A. & Hofmockel, K.S., 2013. Reaction- and Sample-specific Inhibition Affect Standardization of qPCR Assays of Soil Bacterial Communities. *Soil Biology and Biochemistry*, 59, pp.89–97. doi: 10.1016/j.soilbio.2013.01.007.

Hashish, A. et al., 2021. Development and Validation of Two Diagnostic Real-Time PCR (Taqman) Assays for the Detection of Bordetella avium from Clinical Samples and Comparison to the Currently Available Real-Time Taqman PCR Assay. *Microorganisms*, 9, 2232. doi: 10.3390/microorganisms9112232.

Hu, Y. et al., 2012. Glioma Cells Promote the Expression of VCAM-1 on BM-MSCs: a Possible Mechanism for Their Tropism Toward Gliomas. Jo*urnal of Molecular Neuroscience*, 48(1), pp.127–135.

Jiménez, C. et al., 2000. Role of the PI3K Regulatory Subunit in the Control of Actin Organization and Cell Migration. *The Journal of Cell Biology*, 151(2), pp.249–261.

Johnston, A.D. et al., 2019. PrimerROC: Accurate Condition-Independent Dimer Prediction using ROC Analysis. *Scientific Reports*, 9, 209. doi: 10.1038/s41598-018-36612-9.

Kang, S.J. et al., 2021. Comparison of Seven Commercial TaqMan Master Mixes and Two Real-Time PCR Platforms Regarding the Rapid Detection of Porcine DNA. *Food Science of Animal Resources*, 41(1), pp.85–94. doi: 10.5851/KOSFA.2020.E80.

Landry, N.M., Rattan, S.G. & Dixon, I.M.C., 2019. An Improved Method of Maintaining Primary Murine Cardiac Fibroblasts in Two-Dimensional Cell Culture. *Scientific Reports*, 9, 12889. doi: 10.1038/s41598-019-49285-9.

Langlois, V.S. et al., 2021. The Need for Robust qPCR-based eDNA Detection Assays in Environmental Monitoring and Species Inventories. *Environmental DNA*, 3(3), pp.519–527. doi: 10.1002/edn3.164.

Lee, S.B. et al., 2016. Ethyl Acetate Fraction of Amomum xanthioides Exerts Antihepatofibrotic Actions via the Regulation of Fibrogenic Cytokines in a Dimethylnitrosamine-Induced Rat Model. *Evidence-based Complementary and Alternative Medicine*, 2016, 6014380. doi: 10.1155/2016/6014380.

Luna, G.M. et al., 2012. A New Molecular Approach based on qPCR for the Quantification of Fecal Bacteria in Contaminated Marine Sediments. *Journal of Biotechnology*, 157(4), pp.446–453. doi: 10.1016/j.jbiotec.2011.07.033.

Morinha, F., Magalhães, P. & Blanco, G., 2020. Different qPCR Master Mixes Influence Telomere Primer Binding within and between Bird Species. *Journal of Avian Biology*, 51(2), e02352. doi: 10.1111/jav.02352.

Nakano, S.I. et al., 1999. Nucleic Acid Duplex Stability: Influence of Base Composition on Cation Effects. *Nucleic Acids Research*, 27(14), pp.2957–2965. doi: 10.1093/nar/27.14.2957.

Ouldridge, T.E. et al., 2013. DNA Hybridization Kinetics: Zippering, Internal Displacement and Sequence Dependence. *Nucleic Acids Research*, 41(19), pp.8886–8895. doi: 10.1093/nar/gkt687.

Petrovan, V. et al., 2020. Evaluation of Commercial qPCR Kits for Detection of SARS-CoV-2 in Pooled Samples. *Diagnostics*, 10(7), 472. doi: 10.3390/diagnostics10070472.

Ririe, K.M., Rasmussen, R.P. & Wittwer, C.T., 1997. Product Differentiation by Analysis of DNA Melting Curves during the Polymerase Chain Reaction. *Analytical Biochemistry*, 245(2), pp.154–160. doi: 10.1006/abio.1996.9916.

Sato, H. et al., 2021. Downregulation of Mitochondrial Biogenesis by Virus Infection Triggers Antiviral Responses by Cyclic GMP-AMP Synthase. *PLoS Pathogens*, 17(10), e1009841. doi: 10.1371/journal.ppat.1009841.

Sharma, A. et al., 2021. Comparative Transcriptomic and Molecular Pathway Analyses of HL-CZ Human Pro-Monocytic Cells Expressing SARS-CoV-2 Spike S1, S2, NP, NSP15 and NSP16 Genes. *Microorganisms*, 9(6), p.1193. doi: 10.3390/microorganisms9061193.

Singh, V.K. et al., 2000. The Effect of Hairpin Structure on PCR Amplification Efficiency. *Molecular Biology Today*, 1(3), pp.67–69.

Su, Q., Sena-Esteves, M. & Gao, G., 2020. Titration of Recombinant Adeno-Associated Virus (rAAV) Genome Copy Number Using Real-Time Quantitative Polymerase Chain Reaction (qPCR). *Cold Spring Harbor Protocols*, 2020(5), pp.158–161. doi: 10.1101/pdb.prot095646.

Tajima, K. et al., 2001. Diet-Dependent Shifts in the Bacterial Population of the Rumen Revealed with Real-Time PCR. *Applied and Environmental Microbiology*, 67(6), pp.2766–2774. doi: 10.1128/AEM.67.6.2766-2774.2001.

Taylor, S. et al., 2010. A Practical Approach to RT-qPCR-Publishing Data that Conform to the MIQE Guidelines. *Methods*, 50(4), pp.S1–S5. doi: 10.1016/j.ymeth.2010.01.005.

Thornton, B. & Basu, C., 2011. Real-Time PCR (qPCR) Primer Design Using Free Online Software Received. *Biochemistry and Molecular Biology Education*, 39(2), pp.145–154. doi: 10.1002/bmb.20461.

Trigo, B.B. et al., 2021. *In Silico* and *In Vitro* Evaluation of Primers for Molecular Differentiation of Leishmania Species. *Brazilian Journal of Veterinary Parasitology*, 30(1), e022020. doi: 10.1590/s1984-296120201078.

Vanneste, K. et al., 2018. Application of Whole Genome Data for In Silico Evaluation of Primers and Probes Routinely Employed for the Detection of Viral Species by RT-qPCR using Dengue Virus as a Case Study. *BMC Bioinformatics*, 19(1), 312. doi: 10.1186/s12859-018-2313-0.

Vogels, C.B.F. et al., 2020. Analytical Sensitivity and Efficiency Comparisons of SARS-CoV-2 RT–qPCR Primer–Probe Sets. *Nature Microbiology*, 5(10), pp.1299–1305. doi: 10.1038/s41564-020-0761-6.

Von Ahsen, N., Wittwer, C.T. & Schütz, E., 2001. Oligonucleotide Melting Temperatures under PCR Conditions: Nearest-Neighbor Corrections for Mg^{2+}, Deoxynucleotide Triphosphate, and Dimethyl Sulfoxide Concentrations with Comparison to Alternative Empirical Formulas. *Clinical Chemistry*, 47(11), pp.1956–1961. doi: 10.1093/clinchem/47.11.1956.

Vulchi, R., Daane, K.M. & Wenger, J.A., 2021. Development of DNA Melt Curve Analysis for the Identification of Lepidopteran Pests in Almonds and Pistachios. *Insects*, 12(6), 553. doi: 10.3390/insects12060553.

Wang, H. et al., 2019. An Exonuclease-assisted Fluorescence Sensor for Assaying Alkaline Phosphatase based on SYBR Green I. *Molecular and Cellular Probes*, 45, pp.26–30. doi: 10.1016/j.mcp.2019.04.002.

Yang, T., Liu, J. & Chen, J., 2020. Compared with Conventional PCR Assay, qPCR Assay Greatly Improves the Detection Efficiency of Predation. *Ecology and Evolution*, 10(14), pp.7713–7722. doi: 10.1002/ece3.6494.

Ye, J. et al., 2012. Primer-BLAST: A Tool to Design Target-Specific Primers for Polymerase Chain Reaction. *BMC Bioinformatics*, 13, 134. doi: 10.1186/1471-2105-13-134.

In Silico and Validation Approaches for Optimum Conditions of Rattus norvegicus Target Gene qPCR Primers

ORIGINALITY REPORT

9%	6%	6%	4%
SIMILARITY INDEX	INTERNET SOURCES	PUBLICATIONS	STUDENT PAPERS

PRIMARY SOURCES

1	Chrysa Koukorava, Kelly Ward, Katie Ahmed, Sumaya Dauleh et al. " Mesothelial cells exhibit characteristics of perivascular cells in an angiogenesis assay ", Cold Spring Harbor Laboratory, 2023 Publication	1%
2	Submitted to Institut Pertanian Bogor Student Paper	1%
3	www.journal.ugm.ac.id Internet Source	1%
4	researchonline.jcu.edu.au Internet Source	<1%
5	link.springer.com Internet Source	<1%
6	gitea.petton.fr Internet Source	<1%
7	"PCR Primer Design", Springer Science and Business Media LLC, 2022 Publication	<1%

8	www.frontiersin.org Internet Source	<1 %
9	humaniora.journal.ugm.ac.id Internet Source	<1 %
10	www.bio-rad.com Internet Source	<1 %
11	www.antibodyassay.com Internet Source	<1 %
12	Bourzac, Kevin M., Lori J. LaVine, and Margaret S. Rice. "Analysis of DAPI and SYBR Green I as Alternatives to Ethidium Bromide for Nucleic Acid Staining in Agarose Gel Electrophoresis", Journal of Chemical Education, 2003. Publication	<1 %
13	irep.ntu.ac.uk Internet Source	<1 %
14	iubmb.onlinelibrary.wiley.com Internet Source	<1 %
15	Simona Camorani, Billy Samuel Hill, Raffaela Fontanella, Adelaide Greco et al. "Inhibition of Bone Marrow-Derived Mesenchymal Stem Cells Homing Towards Triple-Negative Breast Cancer Microenvironment Using an Anti-PDGFRβ Aptamer", Theranostics, 2017 Publication	<1 %

16	bmcmedgenomics.biomedcentral.com Internet Source	<1 %
17	www.karger.com Internet Source	<1 %
18	Submitted to Royal Holloway and Bedford New College Student Paper	<1 %
19	Submitted to Oxford Brookes University Student Paper	<1 %
20	Jessica D. Stevens, Meghan B. Parsley. " Environmental applications and their associated gene targets for management and conservation ", Environmental DNA, 2022 Publication	<1 %
21	reproductive-health-journal.biomedcentral.com Internet Source	<1 %
22	Timothy Chaya, Aparajita Banerjee, Brian D. Rutter, Deji Adekanye, Jean Ross, Guobin Hu, Roger W. Innes, Jeffrey L. Caplan. " Characterization of extracellular vesicles isolated from reveals a conservation between monocot and eudicot extracellular vesicle proteomes ", Cold Spring Harbor Laboratory, 2023 Publication	<1 %

23	journals.plos.org Internet Source	<1 %
24	H.S. Bennypaul, D.S. Sanderson, P. Donaghy, I. Abdullahi, M. Green, V. Klaassen, M. Al Rwahnih. "Development of a one-step RT-qPCR assay for the detection of Grapevine leafroll-associated virus 7.", Journal of Virological Methods, 2022 Publication	<1 %
25	Mark Pryjma, Jan Burian, Kevin Kuchinski, Charles J. Thompson. " Antagonism between front line antibiotics clarithromycin and amikacin used for the treatment of infections is mediated by the gene ", Antimicrobial Agents and Chemotherapy, 2017 Publication	<1 %
26	www.nature.com Internet Source	<1 %
27	Alescia A. Roberto, Jonathon B. Van Gray, Jean Engohang-Ndong, Laura G. Leff. "Distribution and co-occurrence of antibiotic and metal resistance genes in biofilms of an anthropogenically impacted stream", Science of The Total Environment, 2019 Publication	<1 %
28	Francesco Sambo, Francesca Finotello, Enrico Lavezzo, Giacomo Baruzzo et al. "Optimizing	<1 %

PCR primers targeting the bacterial 16S ribosomal RNA gene", BMC Bioinformatics, 2018
Publication

29 Methods in Molecular Biology, 2015. <1 %
Publication

30 Rapid Cycle Real-Time PCR, 2001. <1 %
Publication

31 www.biorxiv.org <1 %
Internet Source

32 www.ncbi.nlm.nih.gov <1 %
Internet Source

33 Methods in Molecular Biology, 2014. <1 %
Publication

34 Brenda Thornton, Chhandak Basu. "Real-time PCR (qPCR) primer design using free online software", Biochemistry and Molecular Biology Education, 2011 <1 %
Publication

35 Enric Cuevas Ferrando. "Detection and tracking of emerging viruses of public health interest in waters through molecular and metagenomic procedures", Universitat Politecnica de Valencia, 2022 <1 %
Publication

Exclude quotes	On	Exclude matches	Off
Exclude bibliography	On		